ACS APPLIED MATERIALS & INTERFACES

Research Article

www.acsami.org

Flexible Graphene–Graphene Composites of Superior Thermal and Electrical Transport Properties

Zhi-Ling Hou,[†] Wei-Li Song,*[,‡] Ping Wang,[†] Mohammed J. Meziani,*[,§] Chang Yi Kong,[†] Ankoma Anderson,[†] Halidan Maimaiti,[†] Gregory E. LeCroy,[†] Haijun Qian,[†] and Ya-Ping Sun*[,†]

[†]Department of Chemistry and Laboratory for Emerging Materials and Technology, Clemson University, Clemson, South Carolina 29634-0973, United States

[‡]Institute of Advanced Materials and Technology, University of Science and Technology Beijing, Beijing 100083, China

[§]Department of Natural Sciences, Northwest Missouri State University, Maryville, Missouri 64468, United States

Supporting Information

ABSTRACT: Graphene is known for high thermal and electrical conductivities. In the preparation of neat carbon materials based on graphene, a common approach has been the use of well-exfoliated graphene oxides (GOs) as the precursor, followed by conversion to reduced GOs (rGOs). However, rGOs are more suitable for the targeted high electrical conductivity achievable through percolation but considerably less effective in terms of efficient thermal transport dictated by phonon progression. In this work, neat carbon films were fabricated directly from few-layer graphene sheets, avoiding rGOs completely. These essentially graphene–graphene composites were of a metal-like appearance and mechanically flexible, exhibiting superior thermal and electrical transport properties. The observed thermal and electrical conductivities are higher than 220 W/m·K and 85000 S/m, respectively. Some issues in the further development of these mechanically flexible graphene–graphene nanocomposite materials are discussed and so are the associated opportunities.

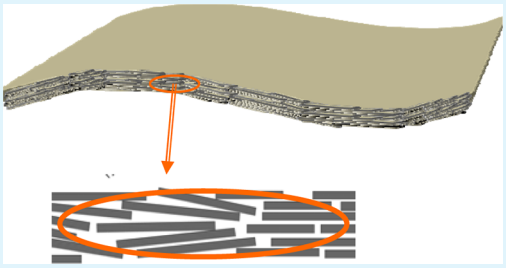

KEYWORDS: *thermal conductivity, electrical conductivity, graphene, composite film, flexible composite, graphene oxide*

INTRODUCTION

Light-weight materials of superior thermal and/or electrical transport properties have received much attention for their variety of technological applications, from the rapidly increasing demand in effective thermal management systems to the enabling technology for high-performance electronics.[1−4] Graphene nanosheets (GNs) are ideally suited for these materials, with the all-carbon two-dimensional configuration and delocalized π-electronic network for excellent thermal and electrical conductivities.[1−3,5−7] For thermal transport, both theoretical and experimental results have suggested in-plane thermal conductivity up to thousands of W/m·K units at the individual graphene sheet level.[5,6,8−10] Therefore, these nanosheets, including especially the few-layer ones, have been widely pursued as fillers in polymeric nanocomposite materials for much enhanced thermal conductivity.[1,11−17] For example, Haddon and co-workers dispersed graphite nanoplatelets into epoxy matrixes to obtain composites of thermal conductivity up to 6.44 W/m·K at 25 vol % filler loading.[11] Veca et al. fabricated flexible nanocomposite films of epoxy polymer with few-layer GNs, with the observed in-plane thermal conductivity close to 80 W/m·K at 33 vol % filler loading.[13] GNs have also been used as filler in polymeric nanocomposites for electrically conductive properties, although the filler loading in these nanocomposites has often been at the lower side. This is probably due to the fact that mechanistically the electrical conductivity is dictated by percolation while the thermal conductivity is associated with phonon propagation (vibrational motion propagating through condensed matter).

The concept and practice on graphene-based composites go beyond the polymeric systems, including also the development of all-carbon nanocomposites from GNs and their derived precursors.[18−22] In targeted thermal transport applications, these nanocomposites are often pursued as an alternative to the highly ordered pyrolytic graphite materials of ultimate performance (the in-plane thermal conductivity of 400−1800 W/m·K, for example).[12,23−26] However, the ordered graphite materials are sometimes limited by other properties, such as their brittle nature not suitable for applications that require flexible structures, and they are generally very high in cost.[24−26] There have been a number of reported strategies on the development of flexible graphene composites with nanoscale structural features.[1,18−22] For example, Xiang and Drzal prepared papers of neat graphite nanoplatelets through mechanical pressing for high thermal transport performance.[19] Further improvements in the performance were achieved by processing the papers in a combination of thermal-annealing and hot-press treatment, reaching an in-plane thermal

Received: May 14, 2014
Accepted: August 13, 2014
Published: August 13, 2014

conductivity of 313 W/m·K.[20] Tian et al. used exfoliated graphene oxides (GOs) for the dispersion of few-layer GNs and also as the precursor for reduced GOs (rGOs).[18] The nanocomposite films thus fabricated were thermally annealed to facilitate the GOs-to-rGOs conversion, which was accompanied by the removal of oxygen-containing groups or species to allow more intimate contacts between rGOs and the embedded few-layer GNs. The resulting essentially all-carbon films exhibited excellent thermal transport properties, with the observed thermal diffusivity (TD) higher than those in aluminum and copper metals.[18] For similar materials of high electrical conductivity, Huang et al. prepared papers from aqueous dispersed graphene sheets that were functionalized with benzenesulfonic acid groups, followed by thermal annealing to reach 44500 S/m in electrical conductivity.[27] Bi et al. fabricated similar papers with somewhat different graphene precursors, which exhibited improved electrical conductivity to 109700 S/m.[28] The use of rGOs for the same purpose has also been popular. Chen et al. prepared GO papers for subsequent chemical reduction and thermal annealing to attain electrical conductivity up to 35100 S/m.[29] The use of large GO sheets as precursors could apparently improve the performance of the resulting papers, according to Lin et al.,[30] with the observed electrical conductivity reaching 139000 S/m after the papers were annealed at a high temperature (1100 °C). However, thermal annealing of GO papers even at relatively low temperatures (such as 200 °C) could degrade their mechanical properties in terms of the paper integrity and flexibility.[29]

In the study reported here, we fabricated flexible nanocomposite films of few-layer graphene sheets directly, without the use of rGOs to avoid their known performance deficiencies in the targeted all-carbon materials. The processed graphene–graphene (GN–GN) composite films, which were of a metal-like appearance and mechanically flexible, exhibited superior thermal and electrical transport properties. The observed thermal and electrical conductivities are higher than 220 W/m·K and 85000 S/m, respectively.

RESULTS AND DISCUSSION

The few-layer GNs were prepared via exfoliation of commercially supplied graphite flakes in a combination of alcohol–water and oxidative acid treatments.[13,18] In the alcohol–water treatment, the as-supplied graphite sample was stirred vigorously and sonicated in an alcohol–water mixture. The sample was then dispersed in a precooled mixture of concentrated nitric acid and sulfuric acid with vigorous sonication. The post-treatment processing included dilution, filtration, and repeated washing of the sample with water until neutral pH was reached. Upon the removal of water and then drying in a vacuum oven, the sample was characterized by using powder X-ray diffraction and Raman spectroscopy. In the former (Figure 1), the diffraction pattern exhibited a broad peak centered at $2\theta \sim 26.5°$, corresponding to the (002) interlayer. According to the Scherrer equation,[31] the peak broadening was consistent with the GNs of an expected average thickness on the order of 10 nm or less. The lateral dimension for the GNs was generally a few microns edge-to-edge based on the optical microscopy results. The Raman spectrum of the GNs was featured with a strong G band and a significant D band (Figure 1), suggesting a meaningful increase of defects from those in the precursor graphite sample.

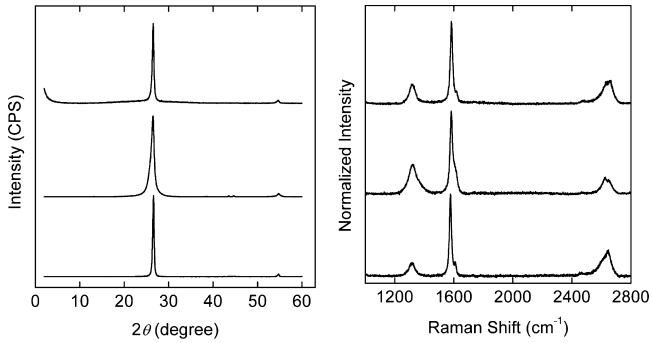

Figure 1. X-ray diffraction patterns (left) and Raman spectra (right) of precursor GNs (bottom in both figures), as-fabricated GN–GN nanocomposite films (middle), and the films post thermal annealing (top).

The GN–GN nanocomposite film fabrication was based on the vacuum filtration method, which has been popular in the preparation of various carbon-nanomaterial-derived film configurations, such as transparent conductive films and "bucky-papers" from carbon nanotubes.[32,33] A number of advantages have been discussed on the use of this method for nanotube films, including a more homogeneous distribution and improved packing of carbon nanotubes in the final films.[33−35] The homogeneity is attributed to the compensation effect naturally associated with the filtration process, such that the already deposited nanotubes reduce the flow of the nanotube suspension to have additional nanotubes deposited into other less dense areas of the film; the packing for improved contacts between nanotubes is credited to the vacuum-pressing in the filtration.[33−35] For the fabrication in this work, the GNs were dispersed in water via homogenization and sonication, and the resulting aqueous suspension was vacuum-filtered through a poly(vinylidene difluoride) (PVDF) filter (0.45 μm pore size) to form a black film on the filter surface. The film was peeled off to be free-standing and then dried in a vacuum oven at 70 °C. As shown in Figure 2, the film thus obtained (around 40 μm in thickness) was mechanically flexible, with a shiny metallic appearance. In the cycling bending test commonly used for evaluating the mechanical flexibility of film materials,[36] the film remained flexible after 50 repeated bending cycles (see also the Supporting Information, SI).

Conceptually, all-carbon films of this kind (Figure 2) are essentially GN–GN nanocomposites, although the basic nanoscale features in this case are at the level of several graphene layers (on the order of a few nanometers in thickness). These features were illustrated in the results from the cross-sectional transmission electron microscopy (TEM) imaging experiments. For TEM imaging, the GN–GN films were microtomed in the direction perpendicular to the film surface for slices of a thickness of less than 100 nm. The TEM images, with representative ones shown in Figure 3, are consistent with the expected film structures of compactly stacked GNs, each of thickness on the order of a few nanometers.

The as-fabricated GN–GN nanocomposite films were evaluated for their thermal transport properties by using a commercially acquired instrument based on the modified laser heating angstrom method,[37,38] measuring the in-plane TD in each film. The accuracy of the instrument for specimen of high TD was evaluated and validated by measuring the standard copper and silver metal films (with known TD values of 117

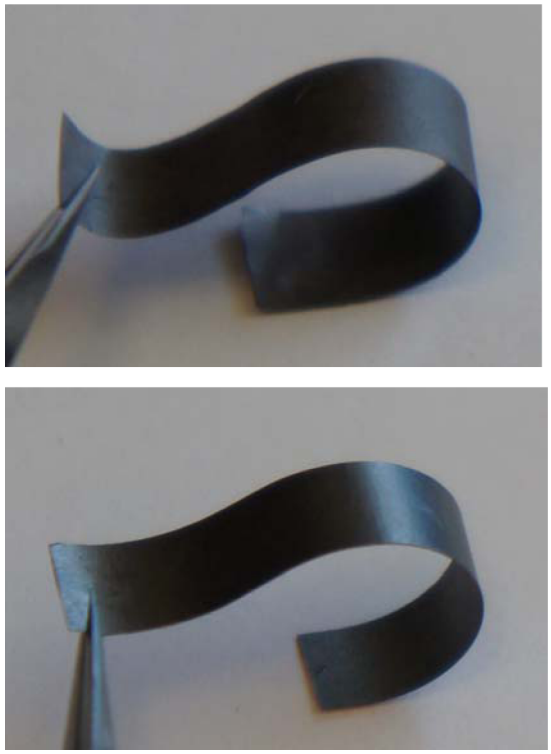

Figure 2. Photographs on a representative as-fabricated GN−GN nanocomposite film (top) and post thermal annealing (bottom). The film dimension was about 5.5 mm × 40 mm.

and 170 mm^2/s, respectively), from which the average deviations with respect to the use of different sets of instrumental parameters and in repeated measurements were generally less than 10%. For the GN−GN nanocomposite films, multiple measurements of several specimens yielded in-plane TD values of 136−174 mm^2/s, averaging 157 mm^2/s (Table 1).

Table 1. Thermal and Electrical Transport Parameters of the GN−GN Nanocomposite Films

sample	TD (mm^2/s)	electrical conductivity (S/m)
GN−GN film	157	70000
annealed GN−GN film	up to 300[a]	85000
rGO film	less than 20	~10000

[a]The value is higher than the calibrated upper limit of the experimental setup.

Theoretically, the thermal conductivity is proportional to the TD with a proportionality constant α, where α = density × specific heat. The experimentally measured density for the film was 1.68 g/cm^3. Therefore, with the commonly used specific heat value of 0.71 J/g·K for such graphitic materials, the average in-plane thermal conductivity of the as-fabricated GN−GN nanocomposite films is on the order of 187 W/m·K.

The thermal transport performance of these GN−GN films is apparently better than that of the previously reported nanocomposite films of GNs dispersed in rGOs.[18] The as-fabricated GN−GN nanocomposite films were also found to be highly electrically conductive, with a experimentally determined (by using the conventional four-probe method) electrical conductivity of about 70000 S/m (Table 1).

The film properties could be improved through thermal-annealing treatment to remove residual oxygen-containing groups and/or species carried over from the precursor GN samples used in the film fabrication. The annealing was at 1060 °C in an inert atmosphere (flowing argon gas) for about 2 h. For post thermal annealing, the shiny metallic appearance of the films was more pronounced, accompanied by a slight

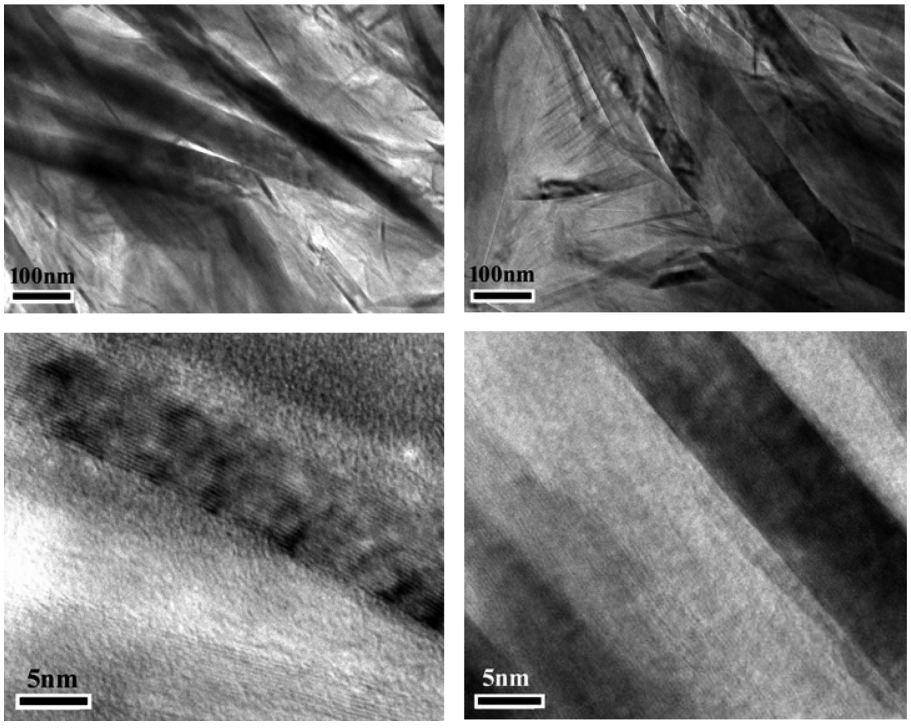

Figure 3. TEM images at lower (top) and higher (bottom) resolution on the slices from microtoming of the as-fabricated (left) and post thermal annealing (right) GN−GN nanocomposite films.

reduction in the film thickness and enhanced mechanical flexibility (Figure 2 and see also the SI). The X-ray diffraction peak of the annealed films became sharper (Figure 1), suggesting an increase (thicker) in the nanoscale features in the GN−GN films postannealing. The increase could be associated with several possible structural changes, including a partial restacking in the individual GN pieces (a reversal of the exfoliation) and an improved stacking between neighboring GN pieces. The latter, conceptually more consistent with the targeted GN−GN nanocomposite structures, should enhance the thermal and electrical transport properties. However, TEM analyses of the specimen from microtoming of the annealed GN−GN films yielded results that could not capture the nanoscale structural changes, with the observed images largely similar to those from the as-fabricated films before the annealing treatment (Figure 3). The Raman spectrum of the annealed films (Figure 1) exhibits a lower D band to G band ratio, consistent with the expected decrease of defects in the GN structures.

A piece of the GN−GN film was twisted until being fractured, and the fractured edge was examined using scanning electron microscopy (SEM). In the SEM image (Figure 4), the relatively well-ordered layer structure in the film is rather obvious.

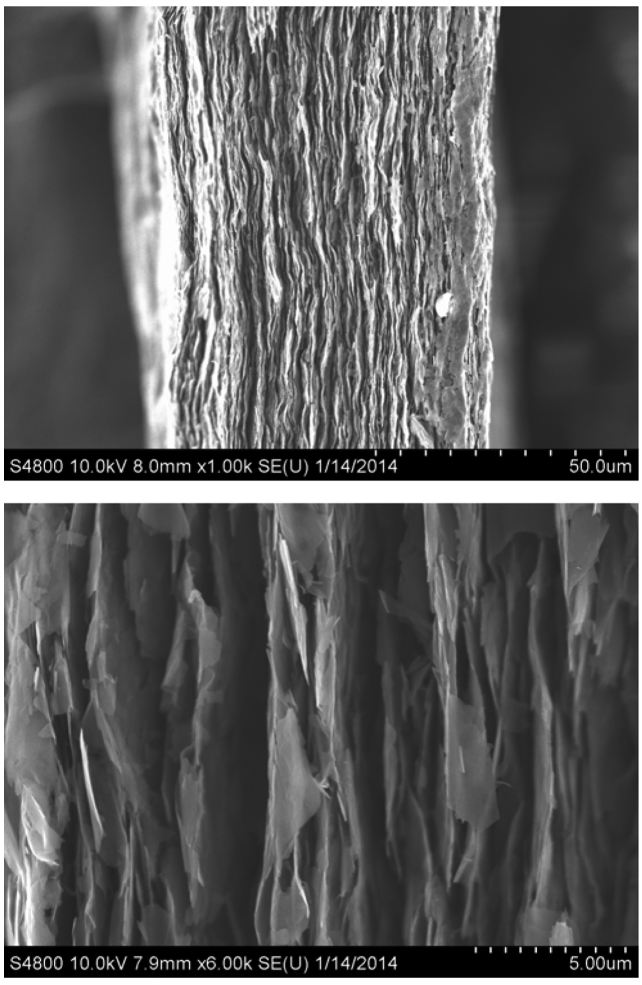

Figure 4. SEM images on the fractured edges of a representative GN−GN nanocomposite film.

X-ray photoelectron spectroscopy (XPS) results on atomic concentrations suggested that the annealed GN−GN film was purer than the graphite starting material in terms of carbon and oxygen contents, 98.3% and 1.7% in the former versus 97% and 3% in the latter, respectively. The as-fabricated film without annealing was not as pure, containing 90.4% carbon, 8.7% oxygen, and 0.9% nitrogen.

In the GN−GN films postannealing, there were indeed significant performance enhancements. The observed electrical conductivity increased more than 20% to 85000 S/m (Table 1). The enhancement in thermal transport was apparently even more substantial, with the observed in-plane TD values as high as 300 mm^2/s (Table 1). However, because the instrument was not designed specifically for such highly thermally conductive specimen (beyond the calibration with the standard silver metal film), the accuracy of the measurements and results could not be confirmed. Nevertheless, the annealed GN−GN nanocomposite films were apparently highly thermally conductive, more so than the standard silver metal film (known TD of 170 mm^2/s). Thus, the in-plane TD in the annealed GN−GN films should be in the range of 170−300 mm^2/s. The annealing also made the films more dense, with an experimentally measured density of 1.83 g/cm^3. Under the assumption of the specific heat being unchanged, which is a common practice in the literature, thermal conductivities of the annealed GN−GN films should be in the range of 220−390 W/m·K. Therefore, the thermal transport performance of these obviously flexible films is close to that found in some commercially supplied pyrolytic graphite materials (which are generally brittle with little mechanical flexibility).[24−26]

Experimentally, the film fabrication from the precursor GNs was relatively simple and stable in terms of being insensitive to unavoidable variations in duplicating preparations, with generally reproducible outcomes. The production of the precursor GNs was also insensitive to changes in the processing conditions (various lengths of sonication time, for example), which, on the one hand, provided stability in terms of yielding the precursor GNs in a relatively consistent fashion but, on the other hand, dampened the prospect of producing GNs of different nanoscale features by varying the processing conditions. In principle, thinner GNs would probably be more advantageous to further performance enhancements in the flexible GN−GN nanocomposite films, as extrapolated from the general desire for a better dispersion of lower-dimensional fillers in nanocomposite materials.[1] For such a purpose, rGOs recovered from well-exfoliated largely single-layer GOs may represent another extreme, namely, for the fabrication of rGO−rGO composite films with the nanoscale feature down to the single-layer rGO level. However, as reported previously[18,39,40] and confirmed in this study, such rGO films converted from GO films through an exhaustive processing effort, including chemical reduction, thermal annealing, etc., and their combinations, are generally poor in thermal transport performance. For example, the TD values for the rGO films with observed electrical conductivity of about 10000 S/m were less than 20 mm^2/s, considerably lower than those found in the GN−GN nanocomposite films discussed above with the few-layer GNs as precursors.

In the literature, rGO films of high electrical conductivity (139000 S/m, for example) have been reported.[30] The thermal conductivity to electrical conductivity ratios should be much lower in those films than in the GN−GN nanocomposite films obtained in this work. This is consistent with the mechanistic

differences between electrical transport and thermal transport in the composite films, which are dictated by the electrical percolation and phonon progression in the filler nanostructures, respectively. The former is obviously more readily established in the conversion from GOs to rGOs; thus, high electrical conductivity in the rGO films is achieved. The GNs without their graphene structures being severely damaged like in GOs are apparently more robust precursors for highly thermally conductive films. The excellent mechanical flexibility and generally facile fabrication from inexpensive precursors make these all-carbon nanocomposite materials very competitive in many applications that demand ultrahigh thermal transport. Further performance enhancements with the use of thinner GNs, for which the production remains a challenge, may be expected.

In summary, few-layer GNs can be produced from the exfoliation of graphite in a relatively simple processing procedure, which is amenable to being scaled up because there is no meaningful bottleneck in the production. The GNs in aqueous dispersion can be fabricated directly into neat carbon films without any involvement of GOs or rGOs, and the resulting materials are essentially GN−GN nanocomposites both conceptually and practically. These unique nanocomposite materials offer superior thermal and electrical transport properties. While the observed electrical conductivity values for the GN−GN nanocomposites are no better than those achieved in well-fabricated rGO films, the thermal transport performance of the GN−GN nanocomposites is considerably more robust. In fact, the thermal conductivity in the GN−GN nanocomposites is close to that found in low-end pyrolytic graphite materials, yet the former (unlike the latter) remains mechanically flexible. Therefore, broad and significant applications of the GN−GN nanocomposites in thermal management and other systems may be envisaged.

EXPERIMENTAL SECTION

Materials. The graphite sample (surface-enhanced flake graphite, grade 3805) was supplied by Asbury Carbons. Sulfuric acid (93%), nitric acid (73%), ethanol, hydrogen peroxide (35%), and phosphorus pentoxide (P_2O_5) were purchased from Acros, ammonium persulfate ($(NH_4)_2S_2O_8$) was purchased from Aldrich, and potassium permanganate ($KMnO_4$) was purchased from Fisher Scientific. Poly(vinylidene difluoride) (PVDF) membrane filters (0.45 μm pore size) were acquired from Fisher Scientific, the dialysis membrane tubing (MWCO $\approx$ 3500) was acquired from Spectrum Laboratories, and carbon-coated copper grids for TEM analyses were acquired from SPI Supplies. Water was deionized and purified by being passed through a Labconco WaterPros water purification system.

Measurements. Powder X-ray diffraction measurements were carried out on a Scintag XDS-2000 powder diffraction system and XPS experiments on a Thermo Fisher Scientific ESCALAB 250xi system. Raman spectra were obtained on a Jobin Yvon T64000 Raman spectrometer equipped with a Melles-Griot 35 mW He−Ne laser source for 633 nm excitation, a triple monochromator, a liquid-nitrogen-cooled Symphony detector, and an Olympus BX-41 microscope. SEM images were acquired on a Hitachi S-4800 field-emission SEM system and TEM images on a Hitachi HD-2000 scanning TEM system and a Hitachi H-9500 TEM system with the specimen on a carbon- or holey-carbon-coated copper grid. In the TEM specimen preparation, a film sample was embedded in epoxy resin, followed by microtoming with the use of a Reichert-Jung Ultracut E microtome with a 30° angle diamond knife at room temperature for slices (cross-sectional with respect to the original film surface) of less than 100 nm thickness.

The in-plane TD of a free-standing thin film was determined on an Ulvac LaserPIT TD/conductivity meter operated at room temperature in a vacuum of 0.01 Pa and with the use of multiple frequencies in the measurements. The copper standard came with the instrument, and the commercially supplied (by Otto Frei Co.) silver film of 0.25 mm thickness was used as a reference sample. All of the film samples being tested were cut into rectangular pieces of 30 mm × 5 mm dimension. Commercially acquired silver paste was used as the binder to connect the specimen being tested with the sensor in the sample holder of the instrument.

The electrical conductivity of a film sample was measured by using the classical four-probe method, with the electrical current (I) and voltage (V) relationship for the film determined on the setup consisting of a multimeter (Keithley 2400 controlled by *Lab Tracer 2.0* software, both from Keithley Instruments) and a multiheight probe (Jandel). The electrical conductivity (σ) value was calculated according to the equation $\sigma = (\ln 2/\pi)(I/V)/d$, where d denotes the film thickness. Multiple spots were chosen in the measurement of each film sample, with the readings averaged for each specimen.

GN−GN Composite Films. The as-supplied graphite sample (average graphitic layer thickness on the order of 20−50 nm according to X-ray diffraction results) was processed in a combination of alcohol and oxidative acid treatments for exfoliation. In a typical experiment, the sample (1 g) was added to an alcohol−water mixture [13:7 (v/v), 400 mL], stirred at room temperature for 2 h, and then sonicated (VWR-250D, 120 W) for another 20 h. The sample was collected via filtration and then dried in a vacuum oven. A portion of the sample (250 mg) was added to a precooled (the temperature kept at less than 30 °C throughout) nitric acid−sulfuric acid mixture [1:3 (v/v), 80 mL] and sonicated in a bath sonicator for 72 h. The mixture was then transferred into water (2 L), followed by stirring at room temperature for 1 h to obtain aqueous dispersed GNs.

In the GN−GN film fabrication, an aqueous suspension of GNs (400 mL) was vacuum-filtered through a PVDF filter (0.45 μm pore size) to form a black film on the filter surface. The whole thing (film + filter) was washed repeatedly with deionized water until neutral pH was reached in the aqueous solution from washing. Then, the film was peeled off to be free-standing, followed by drying in a vacuum oven at about 75 °C.

GOs and Films. The preparation of GOs was based on the Hummers method[41] with minor modification. Briefly, concentrated H_2SO_4 (10 mL) in a 500 mL flask was heated to 80 °C, to which $(NH_4)_2S_2O_8$ (0.9 g) and P_2O_5 (0.9 g) were added. The mixture was stirred until the reagents were completely dissolved. The graphite sample (1 g) was added, and the resulting mixture was heated at 80 °C for 4.5 h. Then, the mixture was cooled to room temperature, diluted with water (250 mL), kept there for about 12 h, and filtered and washed repeatedly with water, followed by drying in a vacuum oven. The solid sample was added to concentrated H_2SO_4 (40 mL) in a 500 mL flask cooled in an ice bath. To the mixture was added slowly $KMnO_4$ (5 g over 40 min), during which the temperature was kept at lower than 10 °C. The reaction mixture, with a change in color from black to greenish brown, was heated at 35 °C for 2 h, followed by dilution with water (85 mL; ***caution!*** *the temperature must be kept at lower than 35 °C throughout*) and further stirring for 2 h. Then, the mixture was poured into a large beaker, to which water (250 mL) and then aqueous H_2O_2 (30%, 10 mL) were added. Bubbles from the aqueous mixture along with a color change to brilliant yellow were observed. After the mixture was allowed to settle for about 12 h, the clear supernatant was decanted, and the sediment was washed repeatedly with aqueous H_2SO_4 (5 wt %)−H_2O_2 (0.5 wt %) and a HCl solution (10 wt %), followed by repeated washing with water until no layer separation observed upon centrifugation. The sample was then dialyzed (MWCO ~ 3500) against water for 7 days to yield a clean aqueous dispersion of GOs. The aqueous GOs thus obtained (acid form) were titrated by aqueous NaOH (0.1 M) until the pH was about 9. The resulting GOs (sodium form) were again dialyzed (MWCO ~ 3500) for 7 days to reach neutral pH. Finally, the aqueous suspension of the GOs was diluted (~0.2 wt %) and sonicated for 30 min to achieve complete exfoliation.

For the fabrication of neat GO films, the aqueous dispersed GOs (50 mg) were similarly vacuum-filtered through a PVDF filter (0.45

μm pore size) to form a dark-colored film on the filter surface. The film was peeled off to be free-standing, followed by drying in a vacuum oven at about 75 °C.

Thermal Annealing. The as-fabricated GN−GN composite films were heated in an inert atmosphere (flowing argon gas) in two steps, first slowly (2 °C/min) to 300 °C and then more quickly (7 °C/min) to 1060 °C, followed by thermal annealing at 1060 °C for 2 h. The same procedure was applied to thermal annealing of the neat GO films.

■ ASSOCIATED CONTENT

Supporting Information

Compiled literature data on electrical and thermal conductivities in graphene composites and details on the flexibility test. This material is available free of charge via the Internet at http://pubs.acs.org.

■ AUTHOR INFORMATION

Corresponding Authors

*E-mail: dexterquest@gmail.com.
*E-mail: meziani@nwmissouri.edu.
*E-mail: syaping@clemson.edu.

Notes

The authors declare no competing financial interest.

■ ACKNOWLEDGMENTS

Financial support from South Carolina Space Grant Consortium (SCSGC) and, in part, from the Air Force Office of Scientific Research (AFOSR) through the program of Dr. Charles Lee is gratefully acknowledged. Z.-L.H. was on leave from Beijing University of Chemical Technology in Beijing, China, and H.M. on leave from Xinjiang University in Urumqi, China, both with visiting scholarships provided by the China Scholarship Council. C.Y.K. was supported by the Excellent Young Researchers Overseas Visit Program of Japan Society for the Promotion of Science and A.A. by NASA through a Graduate Research Fellowship managed by SCSGC.

■ REFERENCES

(1) Song, W.-L.; Veca, L. M.; Anderson, A.; Cao, M.-S.; Cao, L.; Sun, Y.-P. Light-Weight Nanocomposite Materials with Enhanced Thermal Transport Properties. *Nanotechnol. Rev.* **2012**, *1*, 363−376.

(2) Yan, Z.; Liu, G.; Khan, J. M.; Balandin, A. A. Graphene Quilts for Thermal Management of High-Power GaN Transistors. *Nat. Commun.* **2012**, *3*, 827−834.

(3) Balandin, A. A. Thermal Properties of Graphene and Nanostructured Carbon Materials. *Nat. Mater.* **2011**, *10*, 569−581.

(4) Huang, H.; Liu, C. H.; Wu, Y.; Fan, S. S. Aligned Carbon Nanotube Composite Films for Thermal Management. *Adv. Mater.* **2005**, *17*, 1652−1656.

(5) Hu, J.; Ruan, X.; Chen, Y. P. Thermal Conductivity and Thermal Rectification in Graphene Nanoribbons: A Molecular Dynamics Study. *Nano Lett.* **2009**, *9*, 2730−2735.

(6) Ghosh, S.; Bao, W.; Nika, D. L.; Subrina, S.; Pokatilov, E. P.; Lau, C. N.; Balandin, A. A. Dimensional Crossover of Thermal Transport in Few-Layer Graphene. *Nat. Mater.* **2010**, *9*, 555−558.

(7) Chen, S.; Wu, Q.; Mishra, C.; Kang, J.; Zhang, H.; Cho, K.; Cai, W.; Balandin, A. A.; Ruoff, R. S. Thermal Conductivity of Isotopically Modified Graphene. *Nat. Mater.* **2012**, *11*, 203−207.

(8) Kong, B. D.; Paul, S.; Nardelli, M. B.; Kim, K. W. First-Principles Analysis of Lattice Thermal Conductivity in Monolayer and Bilayer Graphene. *Phys. Rev. B* **2009**, *80*, 033406.

(9) Balandin, A. A.; Ghosh, S.; Bao, W.; Calizo, I.; Teweldebrhan, D.; Miao, F.; Lau, C. N. Superior Thermal Conductivity of Single-Layer Graphene. *Nano Lett.* **2008**, *8*, 902−907.

(10) Ghosh, S.; Calizo, I.; Teweldebrhan, D.; Pokatilov, E. P.; Nika, D. L.; Balandin, A. A.; Bao, W.; Miao, F.; Lau, C. N. Extremely High Thermal Conductivity of Graphene: Prospects for Thermal Management Applications in Nanoelectronic Circuits. *Appl. Phys. Lett.* **2008**, *92*, 151911.

(11) Yu, A.; Ramesh, P.; Itkis, M. E.; Bekyarova, E.; Haddon, R. C. Graphite Nanoplatelet−Epoxy Composite Thermal Interface Materials. *J. Phys. Chem. C* **2007**, *111*, 7565−7569.

(12) Yu, A.; Ramesh, P.; Sun, X.; Bekyarova, E.; Itkis, M. E.; Haddon, R. C. Enhanced Thermal Conductivity in a Hybrid Graphite Nanoplatelet—Carbon Nanotube Filler for Epoxy Composites. *Adv. Mater.* **2008**, *20*, 4740−4744.

(13) Veca, L. M.; Meziani, M. J.; Wang, W.; Wang, X.; Lu, F.; Zhang, P.; Lin, Y.; Fee, R.; Connell, J. W.; Sun, Y.-P. Carbon Nanosheets for Polymeric Nanocomposites with High Thermal Conductivity. *Adv. Mater.* **2009**, *21*, 2088−2092.

(14) Liang, Q.; Yao, X.; Wang, W.; Liu, Y.; Wong, C. P. A Three-Dimensional Vertically Aligned Functionalized Multilayer Graphene Architecture: An Approach for Graphene-Based Thermal Interfacial Materials. *ACS Nano* **2011**, *5*, 2392−2401.

(15) Yavari, F.; Fard, H. R.; Pashayi, K.; Rafiee, M. A.; Zamiri, A.; Yu, Z.; Ozisik, R.; Borca-Tasciuc, T.; Koratkar, N. Enhanced Thermal Conductivity in a Nanostructured Phase Change Composite due to Low Concentration Graphene Additives. *J. Phys. Chem. C* **2011**, *115*, 8753−8758.

(16) Chu, K.; Jia, C.-C.; Li, W.-S. Effective Thermal Conductivity of Graphene-Based Composites. *Appl. Phys. Lett.* **2012**, *101*, 121916.

(17) Song, S. H.; Park, K. H.; Kim, B. H.; Choi, Y. W.; Jun, G. H.; Lee, D. J.; Kong, B.-S.; Paik, K.-W.; Jeon, S. Enhanced Thermal Conductivity of Epoxy−Graphene Composites by Using Non-Oxidized Graphene Flakes with Non-Covalent Functionalization. *Adv. Mater.* **2013**, *25*, 732−737.

(18) Tian, L.; Anilkumar, P.; Cao, L.; Kong, C. Y.; Meziani, M. J.; Qian, H.; Veca, L. M.; Thorne, T. J.; Tackett, K. N., II; Edwards, T.; Sun, Y.-P. Graphene Oxides Dispersing and Hosting Graphene Sheets for Unique Nanocomposite Materials. *ACS Nano* **2011**, *5*, 3052−3058.

(19) Xiang, J.; Drzal, L. T. Thermal Conductivity of Exfoliated Graphite Nanoplatelet Paper. *Carbon* **2011**, *49*, 773−778.

(20) Wu, H.; Drzal, L. T. Graphene Nanoplatelet Paper as a Light-Weight Composite with Excellent Electrical and Thermal Conductivity and Good Gas Barrier Properties. *Carbon* **2012**, *50*, 1135−1145.

(21) Yuan, G.; Li, X.; Dong, Z.; Westwood, A.; Cui, Z.; Cong, Y.; Du, H.; Kang, F. Y. Graphite Blocks with Preferred Orientation and High Thermal Conductivity. *Carbon* **2012**, *50*, 175−182.

(22) Lee, W.; Lee, J. U.; Jung, B. M.; Byun, J.-H.; Yi, J.-W.; Lee, S.-B.; Kim, B.-S. Simultaneous Enhancement of Mechanical, Electrical and Thermal Properties of Graphene Oxide Paper by Embedding Dopamine. *Carbon* **2013**, *65*, 296−304.

(23) Slack, G. A. Anisotropic Thermal Conductivity of Pyrolytic Graphite. *Phys. Rev.* **1962**, *127*, 694.

(24) Kastelein, B.; Vanbergen, R. D.; Postma, H.; Meijer, H. C.; Mathu, F. Thermal Conductance of Highly Oriented Pyrolytic-Graphite along the C-Direction at Very Low-Temperatures Including Magnetic-Field Effects. *Carbon* **1992**, *30*, 845−850.

(25) Wu, Z.-S.; Ren, W.; Gao, L.; Liu, B.; Jiang, C.; Cheng, H.-M. Synthesis of High-Quality Graphene with a Pre-Determined Number of Layers. *Carbon* **2009**, *47*, 493−499.

(26) Khlevnoy, B. B.; Samoylov, M. L.; Grigoryeva, I. A.; Ibragimov, N. A.; Shapoval, V. I.; Puzanov, A. V.; Ogarev, S. A. Development of High-Temperature Blackbodies and Furnaces for Radiation Thermometry. *Int. J. Thermophys.* **2011**, *32*, 1686−1696.

(27) Huang, W.; Ouyang, X.; Lee, L. J. High-Performance Nanopapers Based on Benzenesulfonic Functionalized Graphenes. *ACS Nano* **2012**, *6*, 10178−10185.

(28) Bi, H.; Chen, J.; Zhao, W.; Sun, S.; Tang, Y.; Lin, T.; Huang, F.; Zhou, X.; Xie, X.; Jiang, M. Highly Conductive, Free-Standing and Flexible Graphene Papers for Energy Conversion and Storage Devices. *RSC Adv.* **2013**, *3*, 8454−8460.

(29) Chen, H.; Mueller, M. B.; Gilmore, K. J.; Wallace, G. G.; Li, D. Mechanically Strong, Electrically Conductive, and Biocompatible Graphene Paper. *Adv. Mater.* **2008**, *20*, 3557−3561.
(30) Lin, X.; Shen, X.; Zheng, Q.; Yousefi, N.; Ye, L.; Mai, Y.-W.; Kim, J.-K. Fabrication of Highly-Aligned, Conductive, and Strong Graphene Papers Using Ultra Large Graphene Oxide Sheets. *ACS Nano* **2012**, *6*, 10708−10719.
(31) Holzwarth, U.; Gibson, N. The Scherrer Equation versus the 'Debye-Scherrer Equation'. *Nat. Nanotechnol.* **2011**, *6*, 534−534.
(32) Bahr, J. L.; Yang, J. P.; Kosynkin, D. V.; Bronikowski, M. J.; Smalley, R. E.; Tour, J. M. Functionalization of Carbon Nanotubes by Electrochemical Reduction of Aryl Diazonium Salts: A Bucky Paper Electrode. *J. Am. Chem. Soc.* **2001**, *123*, 6536−6542.
(33) Lu, F.; Wang, W.; Fernando, K. A. S.; Meziani, M. J.; Myers, E.; Sun, Y.-P. Metallic Single-Walled Carbon Nanotubes for Transparent Conductive Films. *Chem. Phys. Lett.* **2010**, *497*, 57−61.
(34) Wu, Z. C.; Chen, Z. H.; Du, X.; Logan, J. M.; Sippel, J.; Nikolou, M.; Kamaras, K.; Reynolds, J. R.; Tanner, D. B.; Hebard, A. F.; Rinzler, A. G. Transparent, Conductive Carbon Nanotube Films. *Science* **2004**, *305*, 1273−1276.
(35) Li, W. Z.; Wang, X.; Chen, Z. W.; Waje, M.; Yan, Y. S. Carbon Nanotube Film by Filtration as Cathode Catalyst Support for Proton-Exchange Membrane Fuel Cell. *Langmuir* **2005**, *21*, 9386−9389.
(36) Ha, H.-J.; Kil, E.-H.; Kwon, Y. H.; Kim, J. Y.; Lee, C. K.; Lee, S.-Y. UV-Curable Semi-Interpenetrating Polymer Network-Integrated, Highly Bendable Plastic Crystal Composite Electrolytes for Shape-Conformable All-Solid-State Lithium Ion Batteries. *Energy Environ. Sci.* **2012**, *5*, 6491−6499.
(37) Hakovirta, M.; Vuorinen, J. E.; He, X. M.; Nastasi, M.; Schwarz, R. B. Heat Capacity of Hydrogenated Diamond-Like Carbon Films. *Appl. Phys. Lett.* **2000**, *77*, 2340−2342.
(38) Takahashi, F.; Fujii, K.; Hamada, Y.; Hatta, I. Thermal Diffusivity Measurement of Chemical-Vapor-Deposited Diamond by an AC Calorimetric Method. *Jpn. J. Appl. Phys., Part 1* **2000**, *39*, 6471−6473.
(39) Yu, W.; Xie, H.; Li, F.; Zhao, J.; Zhang, Z. Significant Thermal Conductivity Enhancement in Graphene Oxide Papers Modified with Alkaline Earth Metal Ions. *Appl. Phys. Lett.* **2013**, *103*, 141913.
(40) Hwang, Y.; Kim, M.; Kim, J. Enhancement of Thermal and Mechanical Properties of Flexible Graphene Oxide/Carbon Nanotube Hybrid Films Though Direct Covalent Bonding. *J. Mater. Sci.* **2013**, *48*, 7011−7021.
(41) Hummers, W. S., Jr.; Offeman, R. E. Preparation of Graphitic Oxide. *J. Am. Chem. Soc.* **1958**, *80*, 1339−1339.